

Fig. 3 Results of incompressible numerical calculation ($V_a = 0$).

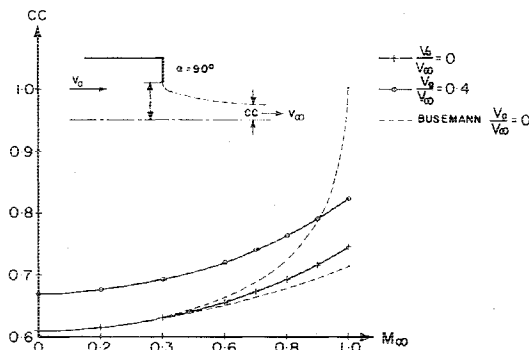


Fig. 4 Contracting coefficient for compressible flow ($\alpha = 90$ deg).

equations⁷:

$$d\left(\frac{x}{L}\right) = \left(\frac{\cos(-\alpha\theta)}{V} \phi_V - \frac{\rho_0}{\rho} \frac{\sin(-\alpha\theta)}{V} \psi_V\right) dV + \left(\frac{\cos(-\alpha\theta)}{V} \phi_\theta - \frac{\rho_0}{\rho} \frac{\sin(-\alpha\theta)}{V} \psi_\theta\right) d\theta \quad (2)$$

$$d\left(\frac{y}{L}\right) = \left(\frac{\sin(-\alpha\theta)}{V} \phi_V + \frac{\rho_0}{\rho} \frac{\cos(-\alpha\theta)}{V} \psi_V\right) dV + \left(\frac{\sin(-\alpha\theta)}{V} \phi_\theta + \frac{\rho_0}{\rho} \frac{\cos(-\alpha\theta)}{V} \psi_\theta\right) d\theta \quad (3)$$

where

$$\phi_V = (\rho_0/\rho) (1 - M^2) / (V\alpha) \psi_\theta \quad (4)$$

$$\phi_\theta = -(\rho_0/\rho) V\alpha \psi_V \quad (5)$$

The reference length L (or the scale factor) is adjusted such that Y_i is unity (Fig. 1). This is accomplished by integrating Eq. (3) from point C first along the constant θ line to any intermediate velocity value and subsequently along the constant velocity line as shown by the dotted line in Fig. 2 until the horizontal axis in the physical plane is reached. The asymptotic height of the jet and the contracting coefficient can be obtained by calculating the freejet boundary starting from point C. It should be remarked that the final asymptotic state occurs only when x approaches infinity. This may be observed from the fact that ψ_V approaches infinity at the asymptotic state D. However, $\sin\theta \psi_V$ approaches zero at this state so that a finite contracting coefficient results as it should.

Figure 3 shows the contracting coefficient for incompressible flow with negligible approaching flow velocity. The agreement with the exact solution, generally within a

fraction of 1% indicates the merit of these calculations. Figure 4 presents the contracting coefficient for compressible flow discharging from an orifice ($\alpha = 90$ deg) for $V_a/V_\infty = 0$ and 0.4. Busemann's original results for $V_a/V_\infty = 0$ from tangent gas approximation are also shown in the same figure. Results for any angle α with different approaching flow velocities can easily be produced. With a relaxation factor of 1.25, one typical set of complete flow calculation takes 0.5 s on the CYBER 175 computing system.

For high-pressure ratios such that the freejet flow is supersonic, additional calculations based on the method of characteristics as suggested by Brown³ may be performed to produce the downstream freejet flowfield and the isoclines obtained from sonic outflow conditions may be employed for these calculations. It is believed that compressible flow calculations for nonsymmetric configurations such as that studied by von Mises for incompressible flow can also be performed by the present scheme of calculations.

Acknowledgment

This work was partially supported by U.S. Army Research Office through research grant No. DAAG29-76-G-0199.

References

- von Mises, R. V., "Berechnung von Ausfluss und Weberfallzahlen," *Zeitschrift für Vereines Deutscher Ingenieure*, Vol. 61, May 1917, p. 447.
- Busemann, A., "Hodographmethode der Gasdynamik," *Zeitschrift für angewandte Mathematik und Mechanik*, Vol. 17, April 1937, p. 73.
- Brown, E. F., "Compressible Flow through Convergent Conical Nozzles with Emphasis on the Transonic Region," Ph.D. Thesis, Department of Mechanical and Industrial Engineering, University of Illinois at Urbana-Champaign, Urbana, Ill., 1968.
- Brown, E. F. and W. L. Chow, "Supercritical Flow through Convergent Conical Nozzles," *Proceedings of the 1st Symposium on Flow: Its Measurement and Control in Science and Industry*, Instrument Society of America, 1974, pp. 231-240.
- Anderson, B. H., "Assessment of an Analytical Procedure for Predicting Supersonic Ejector Nozzle Performance," NASA TN-D-7601, April 1974.
- Anderson, B. H., "Computer Program for Calculating the Flow Field of Supersonic Ejector Nozzles," NASA TN-D-7602, April 1974.
- Shapiro, A. H., *The Dynamics and Thermodynamics of Compressible Fluid Flow*, Vol. 1, The Ronald Press Co., New York, pp. 228-359.

Hypersonic Viscous Shock-Layer Flow over a Highly Cooled Sphere

John D. Waskiewicz,* A. L. Murray,† and Clark H. Lewis‡

Virginia Polytechnic Institute and State University, Blacksburg, Va.

Nomenclature

a, b, c, d, e = coefficients of finite-difference equations
 C_f = skin-friction coefficient, $2\tau_w^*/[\rho^* (U_\infty^*)^2]$

Received Sept. 12, 1977; revision received Oct. 26, 1977. Copyright © American Institute of Aeronautics and Astronautics, Inc. 1977. All rights reserved.

Index categories: Computational Methods; Supersonic and Hypersonic Flow; Viscous Nonboundary-Layer Flows.

*Research Fellow, Aerospace and Ocean Engineering Department.

†Research Associate, Aerospace and Ocean Engineering Department, Student Member AIAA.

‡Professor, Aerospace and Ocean Engineering Department, Associate Fellow AIAA.

| | |
|--------------------|--|
| C_p^* | = specific heat at constant pressure |
| H | = total enthalpy, $H^*/(U_\infty^*)^2$ |
| h_1 | = shape factor in longitudinal direction, $h_1 = 1 + \kappa_L y$ |
| h_3 | = shape factor in transverse direction, $h_3 = r(1 + \kappa_T y \cos \theta_{BL}) / \cos \theta_{BT}$ |
| M_∞ | = freestream Mach number |
| p | = pressure, $p^*/[\rho_\infty^* (U_\infty^*)^2]$ |
| \dot{q} | = heat transfer, $\dot{q}^*/[\rho_\infty^* (U_\infty^*)^3]$ |
| r | = nondimensional axisymmetric radius measured to a point on the body surface, r^*/R_n^* |
| R_n^* | = body nose radius of curvature |
| Re_{∞, R_n} | = freestream Reynolds number based on R_n^* |
| s | = surface distance coordinate measured along the body, s^*/R_n^* |
| St | = Stanton number, $\dot{q}_w / (H_\infty - H_w)$ |
| T | = temperature, $T^*/[U_\infty^*]^2 / C_p^*$ |
| u | = streamwise velocity component tangent to body surface, u^*/U_∞^* |
| v | = velocity component normal to body surface, v^*/U_∞^* |
| w | = transverse velocity component tangent to body surface, w^*/U_∞^* |
| y | = coordinate measured normal to the body, y^*/R_n^* |
| γ | = ratio of specific heats |
| ϵ | = perturbation parameter, $\{\mu^*[(U_\infty^*)^2 / C_p^*] / [\rho_\infty^* U_\infty^* R_n^*]\}^{1/2}$ |
| κ_L | = longitudinal nondimensional surface curvature |
| κ_T | = transverse nondimensional surface curvature |
| μ | = coefficient of viscosity, $\mu^*/\mu^*[(U_\infty^*)^2 / C_p^*]$ |
| θ_{BL} | = body angle, longitudinal direction |
| θ_{BT} | = angle between the body tangent and a line normal to the radius (zero for axisymmetric bodies) |
| ϕ | = transverse or crossflow direction |
| ρ | = density, ρ^*/ρ_∞^* |
| τ^* | = shear stress |
| Superscript | |
| * | = dimensional quantities |
| Subscripts | |
| i | = grid-point counter in s direction |
| j | = grid-point counter in y direction |
| k | = grid-point counter in ϕ direction |
| w | = wall value |
| sh | = value behind the bow shock wave |
| ∞ | = freestream condition |
| MN | = normal momentum equation |
| C | = continuity equation |

Introduction

SOLUTIONS to the viscous shock-layer (VSL) set of equations have been plagued with a major difficulty since the technique was developed by Davis.¹ To obtain solutions, the traditional approach has been to solve each equation separately—a method known as the cascading scheme.²⁻⁴ Few problems have been encountered in finding solutions to the energy and tangential momentum equations since they are second-order parabolic equations. The greatest difficulty has always existed in solving the two first-order equations for continuity and normal momentum. Instabilities introduced by these two equations, which grow in the streamwise direction, have prevented researchers from obtaining solutions far downstream on geometries such as spheres. Until now the method used to obtain solutions further along the body has been relaxation. However, this method fails at a point where instabilities require weighting factors (weighting a fraction of the previous iteration with the current iteration) to closely approach unity (e.g., factors of 0.99 have been used in some applications discussed in Ref. 5). An alternative to the cascading scheme is to couple the solution of the equations. A fully coupled system of all equations would require inversion of large matrices and, hence, would increase the storage

requirements and computation time. A more desirable alternative is to couple only the first-order equations. This procedure will directly eliminate the instability problem and, since the method lends itself to solution by the Thomas Algorithm, the technique will not increase storage requirements nor computation time.

Analysis

The complete, perfect-gas viscous shock-layer equations and a description of the general technique for solving the two-dimensional and axisymmetric flow equations may be found in Ref. 1. Of primary interest to this study are the three-dimensional continuity and normal momentum equations.

$$\frac{\partial}{\partial s} (h_3 \rho u) + \frac{\partial}{\partial y} (h_1 h_3 \rho v) + \frac{\partial}{\partial \phi} (h_1 \rho w) = 0$$

$$\frac{\rho u}{h_1} \frac{\partial v}{\partial s} + \rho v \frac{\partial u}{\partial y} + \frac{\rho w}{h_3} \frac{\partial v}{\partial \phi} - \frac{\rho u^2}{h_1} \frac{\partial h_1}{\partial y} - \frac{\rho w^2}{h_3} \frac{\partial h_3}{\partial y} + \frac{\partial p}{\partial y} = 0$$

The unknowns to be obtained from the solution of this coupled set are pressure p and normal velocity v . To do this, it is necessary to eliminate the density through use of the equation of state. The equations could be written in terms of the density, but for a very cold wall density gradients are large and boundary conditions become a problem. Therefore, this study has found pressure to be a more desirable solution variable. The resulting equations in terms of p and v are

$$\frac{\partial}{\partial s} \left(h_3 \frac{\rho u}{T} \right) + \frac{\partial}{\partial y} \left(h_1 h_3 \frac{\rho v}{T} \right) + \frac{\partial}{\partial \phi} \left(h_1 \frac{\rho w}{T} \right) = 0$$

$$\frac{p u}{T h_1} \frac{\partial v}{\partial s} + \frac{p v}{T} \frac{\partial u}{\partial y} + \frac{p w}{T h_3} \frac{\partial v}{\partial \phi} - \frac{p u^2}{T h_1} \frac{\partial h_1}{\partial y} - \frac{p w^2}{T h_3} \frac{\partial h_3}{\partial y} + \frac{\gamma - 1}{\gamma} \frac{\partial p}{\partial y} = 0$$

To solve the coupled first-order equations, it is necessary to write these equations in a finite-difference form. Derivatives are expressed as follows:

$$\frac{\partial W}{\partial s} = \frac{W_{i,j,k} - W_{i-1,j,k}}{s_i - s_{i-1}}$$

$$\frac{\partial W}{\partial y} = \frac{W_{i,j+1,k} - W_{i,j,k}}{y_{j+1} - y_j}$$

$$\frac{\partial W}{\partial \phi} = \frac{(W_{i-1,j,k+1} - W_{i-1,j,k}) + (W_{i,j,k} - W_{i,j,k-1})}{2(\phi_k - \phi_{k-1})}$$

where W is p or v .

Note that in the interest of clarity the subscript k will be eliminated from the finite difference equations to follow. Since a box scheme is to be used, each equation must be written at both $(j + 1/2)$ and $(j - 1/2)$. The result is a set of four equations to be solved simultaneously, having the form:

$$a_{NM,j+1/2} v_{i,j+1} + b_{NM,j+1/2} v_{i,j} + c_{NM,j+1/2} p_{i,j+1} + d_{NM,j+1/2} p_{i,j} = e_{NM,j+1/2} \quad (1)$$

$$a_{C,j+1/2} v_{i,j+1} + b_{C,j+1/2} v_{i,j} + c_{C,j+1/2} p_{i,j+1} + d_{C,j+1/2} p_{i,j} = e_{C,j+1/2} \quad (2)$$

$$a_{NM,j-1/2} v_{i,j} + b_{NM,j-1/2} v_{i,j-1} + c_{NM,j-1/2} p_{i,j} + d_{NM,j-1/2} p_{i,j-1} = e_{NM,j-1/2} \quad (3)$$

$$a_{C,j-1/2} v_{i,j} + b_{C,j-1/2} v_{i,j-1} + c_{C,j-1/2} p_{i,j} + d_{C,j-1/2} p_{i,j-1} = e_{C,j-1/2} \quad (4)$$

To solve this set of equations, we first eliminate $v_{i,j+1}$ from Eqs. (1 and 2), yielding:

$$k_1 v_{i,j} + k_2 p_{i,j+1} + k_3 p_{i,j} = k_4 \quad (5)$$

where

$$k_1 = a_{C,j+1/2} b_{NM,j+1/2} - a_{NM,j+1/2} b_{C,j+1/2}$$

$$k_2 = a_{C,j+1/2} c_{NM,j+1/2} - a_{NM,j+1/2} c_{C,j+1/2}$$

$$k_3 = a_{C,j+1/2} d_{NM,j+1/2} - a_{NM,j+1/2} d_{C,j+1/2}$$

$$k_4 = a_{C,j+1/2} e_{NM,j+1/2} - a_{NM,j+1/2} e_{C,j+1/2}$$

Similarly, we eliminate $v_{i,j-1}$ from Eqs. (3 and 4), yielding:

$$k_5 v_{i,j} + k_6 p_{i,j} + k_7 p_{i,j-1} = k_8 \quad (6)$$

where

$$k_5 = b_{C,j-1/2} a_{NM,j-1/2} - b_{NM,j-1/2} a_{C,j-1/2}$$

$$k_6 = b_{C,j-1/2} c_{NM,j-1/2} - b_{NM,j-1/2} c_{C,j-1/2}$$

$$k_7 = b_{C,j-1/2} d_{NM,j-1/2} - b_{NM,j-1/2} d_{C,j-1/2}$$

$$k_8 = b_{C,j-1/2} e_{NM,j-1/2} - b_{NM,j-1/2} e_{C,j-1/2}$$

We now eliminate $v_{i,j}$ from Eqs. (5 and 6), yielding:

$$A p_{i,j+1} + B p_{i,j} + C p_{i,j-1} = D$$

where

$$A = k_5 k_2 \quad C = -k_1 k_7$$

$$B = k_5 k_3 - k_1 k_6 \quad D = k_5 k_4 - k_1 k_8$$

The resulting equation may be solved straightforwardly, using the Thomas Algorithm, to write

$$p_{i,j} = E_{pj} p_{i,j-1} + F_{pj}$$

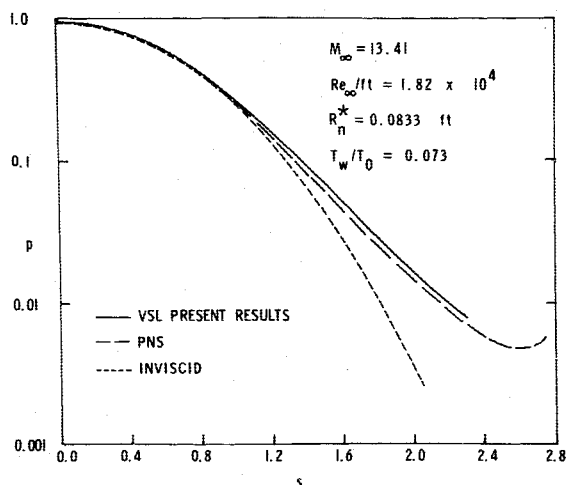


Fig. 1 Surface pressure distributions over a sphere under laminar hypersonic cold-wall conditions.

where

$$E_{pj} = -A / (C E_{pj-1} + B)$$

$$F_{pj} = (D - C F_{pj-1}) / (C E_{pj-1} + B)$$

This procedure may be repeated to yield $v_{i,j}$ by eliminating the pressure rather than the normal velocity.

Results and Discussion

The coupling technique presented here has been successfully implemented in a perfect-gas viscous shock-layer code. The second-order parabolic equations are solved separately, and their solutions are combined with the coupled technique. This has added a great deal of stability to the solution procedure. Previous attempts to obtain solutions on a sphere using the cascading approach failed near $s=1.1$. Use of the coupling technique has permitted solutions which approach separation to be obtained on the back side of the sphere without a noticeable increase in computing time per iteration.

For the purpose of this study we consider a sphere placed in a flow at Mach 13.41. The case is low density ($Re_{\infty, R_n} = 1515$) with an extremely cold wall ($T_w/T_0 = 0.073$). Results include surface pressure distribution, shock standoff distance, skin friction, and wall heat-transfer coefficient data. For com-

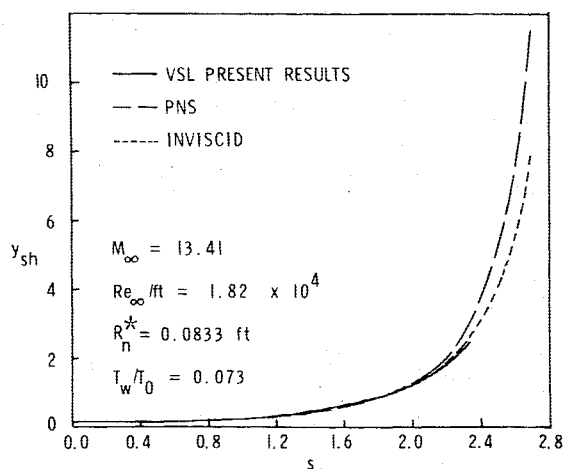


Fig. 2 Shock-layer thickness over a sphere at Mach 13.41 under laminar hypersonic cold-wall conditions.

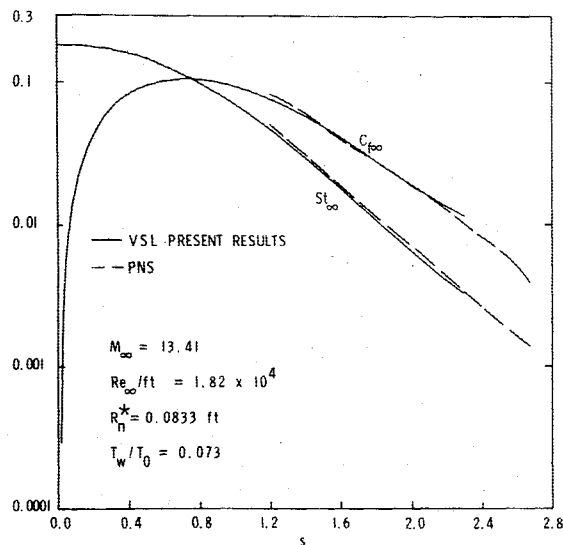


Fig. 3 Skin-friction and heat-transfer distributions over a sphere at laminar hypersonic cold-wall conditions.

parison purposes, both inviscid and parabolized Navier-Stokes (PNS) solutions are also shown. Since the PNS solution procedure cannot be used in the subsonic region near the forward stagnation point, the PNS solution was started with the VSL solution at $s = 1.04$, where the Mach number in the outer, nearly inviscid region was supersonic. Figure 1 gives the pressure distributions from each solution. Agreement between the shock layer and PNS is very good. Figure 2 shows the predicted shock standoff distance. Again, agreement is very good except far downstream on the sphere where the shock-layer thickness grows extremely rapidly. Finally, Fig. 3 presents the skin-friction and wall heat-transfer distributions which also are in excellent agreement.

The results of this study indicate that coupling of the two first-order equations provides substantial improvement in both solution capability and quality over the cascading approach while retaining the advantage of shorter computing time over the fully coupled system. For the case treated here, the complete VSL solution $0 \leq s \leq 2.3$ required 3.00 minutes, and the PNS solution in the range $1.04 \leq s \leq 2.6$ required 30.0 minutes for both solutions on an IBM 370/158 computer.

Where applicable, the VSL technique provides excellent predictions in substantially less computing time than the PNS requires.

References

- ¹Davis, R. T., "Numerical Solution to the Hypersonic Viscous Shock-Layer Equations," *AIAA Journal*, Vol. 8, May 1970, pp. 843-851.
- ²Miner, E. W. and Lewis, C. H., "Hypersonic Ionizing Air Viscous Shock-Layer Flows over Sphere Cones," *AIAA Journal*, Vol. 13, Jan. 1975, pp. 80-88; see also NASA CR-2550, 1975.
- ³Davis, R. T. and Nei, Y. W., "Numerical Solution to the Viscous Shock-Layer Equations for Flow Past Spheres and Paraboloids," Sandia Corp., Albuquerque, N.M., Final Report, Contract No. 48-9195.
- ⁴Whitehead, R. E. and Davis, R. T., "Numerical Solutions to the Viscous Shock-Layer Blunt Body Problem with Inert Gas Injection," Sandia Corp. Report SC-CR-70-6162; Virginia Polytechnic Institute and State University, Jan. 1971.
- ⁵Srivastava, B. N., Werle, M. J., and Davis, R. T., "Viscous Shock Layer Solutions for Hypersonic Sphere-Cones," *AIAA Paper* 77-693, Albuquerque, N.M., June 1977.

From the AIAA Progress in Astronautics and Aeronautics Series . . .

SATELLITE COMMUNICATIONS: FUTURE SYSTEMS-v. 54 ADVANCED TECHNOLOGIES-v. 55

Edited by David Jarett, TRW, Inc.

Volume 54 and its companion Volume 55, provide a comprehensive treatment of the satellite communication systems that are expected to be operational in the 1980's and of the technologies that will make these new systems possible. Cost effectiveness is emphasized in each volume, along with the technical content.

Volume 54 on future systems contains authoritative papers on future communication satellite systems in each of the following four classes: North American Domestic Systems, Intelsat Systems, National and Regional Systems, and Defense Systems. **A significant part of the material has never been published before.** Volume 54 also contains a comprehensive chapter on launch vehicles and facilities, from present-day expendable launch vehicles through the still developing Space Shuttle and the Intermediate Upper Stage, and on to alternative space transportation systems for geostationary payloads. All of these present options and choices for the communications satellite engineer. The last chapter in Volume 54 contains a number of papers dealing with advanced system concepts, again treating topics either not previously published or extensions of previously published works.

Volume 55 on advanced technologies presents a series of new and relevant papers on advanced spacecraft engineering mechanics, representing advances in the state of the art. It includes new and improved spacecraft attitude control systems, spacecraft electrical power, propulsion subsystems, spacecraft antennas, spacecraft RF subsystems, and new earth station technologies. Other topics are the relatively unappreciated effects of high-frequency wind gusts on earth station antenna tracking performance, multiple-beam antennas for higher frequency bands, and automatic compensation of cross-polarization coupling in satellite communication systems.

With the exception of the first "visionary" paper in Volume 54, all of these papers were selected from the 1976 AIAA/CASI 6th Communication Satellite Systems Conference held in Montreal, Canada, in April 1976, and were revised and updated to fit the theme of communication satellites for the 1980's. These archive volumes should form a valuable addition to a communication engineer's active library.

*Volume 54, 541 pp., 6×9, illus., \$19.00 Mem., \$35.00 List
Volume 55, 489 pp., 6×9, illus., \$19.00 Mem., \$35.00 List
Two-Volume Set (Vols. 54 and 55), \$55.00 Mem. & List*

TO ORDER WRITE: Publications Dept., AIAA, 1290 Avenue of the Americas, New York, N. Y. 10019